공학석사학위논문

Efficient co-delivery of doxorubicin and gold nanorod in PLGA nanoparticles coated by TNF-a-treated MSC membrane for cancer treatment

암 치료를 위한 세포막으로 코팅된 독소루비신과 금나노로드가 함유된 PLGA 나노입자 개발

2016년 8월

서울대학교 대학원
화학생물공학부
오 재 서

Efficient co-delivery of doxorubicin and gold nanorod in PLGA nanoparticles coated by TNF-atreated MSC membrane for cancer treatment

암 치료를 위한 세포막으로 코팅된 독소루비신과 금나노로드가 함유된 PLGA 나노입자 개발

지도 교수 김 병 수

이 논문을 공학석사 학위논문으로 제출함

2016년 8월

서울대학교 대학원

화학생물공학부

오재서

오재서의 석사 학위논문을 인준함

2016년 8월

위 원 장 백승렬 (인)

부 위 원 장 김병수 (인)

위 원 김병기 (인)

Abstract

Efficient co-delivery of doxorubicin and gold nanorod in PLGA nanoparticles coated by TNF-a-treated MSC membrane for cancer treatment

Jaesur Oh
School of Chemical and Biological Engineering
The Graduate School
Seoul National University

Bone marrow-derived mesenchymal stem cells (MSCs) have been extensively studied for cancer therapy using its homing characteristic to injury and tumor tissues. However, MSCs or MSC-derived exosomes would promote tumor growth. To eliminate this risk and take advantage of MSCs, we separated MSC membranes and coated doxorubicin-gold nanorod-PLGA nanoparticles with the membranes (MMNPs). TNF-α-treated MSCs and endothelial cells near tumor shows upregulated vascular cell adhesion molecule-1 (VCAM-1) and very late antigen-4 (VLA-4) on the cell surface. Since VCAM-1 interacts with VLA-4, TNF-α-treated MMNPs (TNF-α MMNPs) exhibited superior tumor vasculature targeting to the polymeric particles or normal MMNPs. Temperature increase by NIR irradiation caused apoptosis of endothelial cells and adjacent

cancer cells, and the nanoparticles flowed into deeper cancer cells leading to death of them.

Keywords: cancer therapy, tumor vasculature, TNF-α, cellular membrane, targeted drug delivery

Student Number: 2014-22612

Contents

List of Figures

HUVEC or normal HUVEC. The nuclei and the membranes of HUVECs were dyed with DAPI (blue) and DiO (green) respectively. DOX is intrinsically red fluorescent. Scale bar: 20 μm.

Figure 6. (a) Real-time infrared thermal images during irradiation to HUVECs or TNF-α MMNPs treated TNF-α HUVECs for 5 minutes. (b) Scheme of co-cultured HUVECs and HT 1080 treated TNF-α treated MMNPs and then infrared irradiation. (c) Temperature increases of each group after 5 minute of irradiation (n = 3). (d) The graph is a MMT assay result showing viability of normal HUVECs and HT 1080s, irradiated HUVECs and HT 1080s, and HUVECs and HT 1080 treated TNF-α treated MMNPs with infrared irradiation.

Figure 7. (a) Real-time infrared thermal images after irradiation for 5 minutes. (b) Scheme of HUVECs and HT 1080s. HUVECs were cultured on transwells. (c) Temperature increases of each group after 5 minute of irradiation (n = 3). TMTH: TNF-α treated HUVECs with TNF-α treated MMNPs, NMTH: TNF-α treated HUVECs with TNF-α untreated MMNPs, TMNH: HUVECs with TNF-α treated MMNPs, NMNH: HUVECs with TNF-α untreated MMNPs. (d) Relative cancer cell viability via MTT assay.

1. Introduction

Over the past decades, bone marrow-derived mesenchymal stem cells (MSCs) have been investigated extensively in biomedicine area due to its outstanding characteristics including self-renewal and wide differentiation variety (1). MSCs were also used in drug delivery system since MSCs tend to home and integrate into injury and tumor sites (1). Although the accurate mechanism of MSC migration is still an unsolved challenge, some of the key parts are revealed: integrin interactions, extracellular matrix interactions, CXCR4 expression and so on (2, 3, 4). In the case of integrin interactions in MSC homing, very late antigen-4 (VLA-4), composed of integrin α4 and integrin β1 on MSCs, binds to vascular cell adhesion molecule-1 (VCAM-1), which is an endothelial ligand interacting with integrinsα4β1 or integrin β1 (4). Furthermore, activated endothelial cells and MSCs in response to tumor necrosis factor-α (TNF-α) stimulation express upregulation of both VCAM-1 and VLA-4 (5, 6, 7). This process enhances the adhesion of MSCs to the endothelium at tumor site.

MSC itself or MSC-derived exosomes, however, would promote tumor growth. In a previous study, MSCs actively migrate to tumors and were stimulated by cancer cells, secreting the chemokine CCL5 (RANTES) (8). This chemokine affects cancer cells in a paracrine way by enhancing the motility, invasion and metastasis of the cancer cells. MSC-derived exosomes also increased the expression of vascular endothelial growth factor (VEGF) in cancer cells by triggering extracellular signal-regulated kinase 1/2 (ERK 1/2) (9). This interaction of MSC-derived exosomes and cancer cells may induce tumor progression.

Cellular membrane utilization is a newly method in top-down approaches, replicating the intrinsic surface characteristics of source cells (10, 11, 12, 13).

Cell membrane-coated nanoparticles are suitable for targeted drug delivery in variable situations with source cell regulation (14).

Gold nanoparticles including GNR have been widely studied as a photothermal agent in the treatment of cancer (15, 16). In this study, Doxorubicin (DOX) and gold nanorod (GNR) were co-loaded in biodegradable poly(lactic-co-glycolic acid) (PLGA) nanoparticles (DOX-GNR-loaded NPs) (16, 17, 18). DOX-GNR-loaded NPs were coated with TNF-α treated MSC membranes (TNF-α MMNPs) to exclude flaws and derive the benefit of MSCs, tumor vasculature targeting (Figure 1). Herein, we hypothesized that TNF-α MMNPs, delivered into targeting sites, would generate heat upon near-infrared (NIR) laser. This will cause irreversible damage to tumor vasculature and cancer cells near the blood vessels. Following this process, TNF-α MMNPs will escape from the endothelial cells and flow into deeper tumors. Release of DOX will lead to apoptosis of the cancer cells.

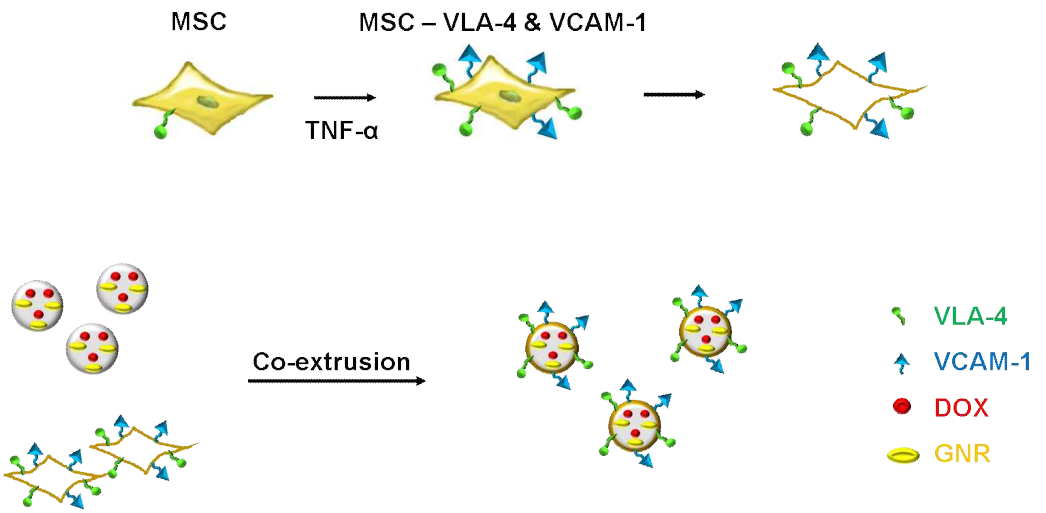

Figure 1. Schematic of MSC membrane separation and TNF-α MMNPs synthesis by extrusion.

2. Experimental section

2.1 Materials

PLGA (M_W = 7,000-17,000), DOX, GNR polyvinyl alcohol (PVA, Sigma-Aldrich, USA), and ethylenediaminetetraacetic acid (EDTA) were obtained from Sigma-Aldrich, USA. Thiazolyl blue tetrazolium bromide (MTT) was also purchased from Sigma-Aldrich, and dichloromethane (DCM) were purchased from J.T.Baker (USA). Dulbecco's Modified Eagle's Medium (DMEM), Endothelial Cell Growth Medium-2 (EGM-2) kit, and fetal bovine serum were purchased from Lonza (USA). Fetal bovine serum (FBS) and penicillin streptomycin (PS) were obtained from Gibco BRL, USA. Sucrose, HEPES, KCl, $MgCl_2$, EDTA, DTT, and PI Cocktail (III) were purchased from Sigma-Aldrich, USA.

2.2 Cell Lines

Human MSCs (hMSCs) in passage number 4 and human endothelial cells (HUVEC) were purchased from Lonza (USA). Human fibrosarcoma cell line (HT-1080) were obtained from American Type Culture Collection (ATCC; USA). MSCs and HT-1080 cells were grown in DMEM supplemented with 10 % (v/v) of FBS and 1 % (v/v) of PS. HUVECs were cultured in EGM-2. The cells were incubated at 37 ℃ with 5 % of CO_2, and DMEM and EGM-2 were changed every two days.

2.3 Preparation of DOX-GNR-loaded PLGA Nanoparticles

10 mg of PLGA and 250 μg of DOX were dissoved in 2 ml DCM. DCM solution was added dropwise to 2 ml of 2.5 % vortexing PVA solution with 500 μg GNR, and then the mixed solution was sonicated for 20 seconds on ice. Solvent was removed by magnetic stirring for 3 hours in 0.3 % PVA at room temperature (RT), and the nanoparticles were washed three times with deionized water by means of centrifugation at 14,000 rpm for 30 minutes. The nanoparticles were lyophilized and stored at －20 ℃.

2.4 DOX-GNR-PLGA Nanoparticle Size and Loading Yield

The size distribution of DOX-GNR-loaded NPs was analyzed by dynamic light scattering spectrophotometer (DLS, DLS-7000, Otsuka Electronics, Japan). DOX-GNR-loaded NPs were dispersed in deionized water for the DLS method.

To figure out the amount of DOX in DOX-GNR-loaded NPs, the amount of DOX in supernatant after the first 14,000 rpm before washing was measured by fluorometer. DOX amount in the supernatant was calculated and subtracted from initial amout of DOX (250ug), which was speculated as DOX amount in in DOX-GNR-loaded NPs.

Quantification of GNR amount in DOX-GNR-loaded NPs was conduced by ICP-AES. DOX-GNR-loaded NPs were lysed with 3 ml aqua regina, and then the gold amount in the nanoparticles was determined via ICP-AES (Thermo Electron Co.).

2.5 Laser Irradiation and Photothermal Imaging of Nanoparticles

DOX-GNR-loaded NPs and PLGA nanoparticles without GNR (DOX-loaded NPs) were dispersed in 100 μl of PBS respectively, and each sample was irradiated using a 660nm CW laser beam for 5 minutes at a power density of 2 W/cm^2. The temperature variations and photothermal images of DOX-GNR-loaded NPs and DOX-loaded NPs were recorded every minute using an infrared thermal imaging system (FLIR i2, FLIR Sustems InC.).

2.6 MMNP Synthesis and Characterization

Before coating process, MSC membranes were separated from MSCs. MSCs grown in 3 dishes of 150mm plate were treated with TNF-α in 10 ng/ml concentration for 48 hours. The cells were detached with 5mM EDTA in PBS and washed two times in PBS 500g. The cells were suspended in 10 ml of subcellular fraction buffer consisting of 250 mM Sucrose, 20 mM HEPES (pH 7.4), 10 mM KCl, 1.5 mM $MgCl_2$, 1 mM EDTA, 1mM DTT, and PI Cocktail (III). The cell solution was disrupted using a homogenizer for 20 times of up-and-down in ice and spun down at 800g for 5 min. The supernatant was saved while the pellet, which included nuclei and unbroken cells, was resuspended in the buffer. The buffer solution was disrupted 20 times of up and down and spun down again. Collected supernatant was centrifuged at 10,000g for 20 min and then the supernatant of 10,000g centrifugation was centrifuged again at 100,000g. The pellet, containing the plasma membrane material, was collected and dispersed in PBS.

To synthesize MMNPs, collected MSC membranes above was extruded through a 400nm polycarbonate membrane for 11 times. The resulting membrane vesicles were then coated onto DOX-GNR-loaded NPs by co-extruding membrane vesicles and DOX-GNR-loaded NP cores through a 400nm polycarbonate membrane for 11 times.

To verify membrane coating on the nanoparticles, ELS, TEM, and confocal microscopy were conducted. First of all, he surface charges of DOX-GNR-loaded NPs, membrane vesicles (MV), and MMNPs were measured using an electrophoretic light-scattering spectrophotometer (ELS-8000, Otsuka Electronics, Osaka, Japan)

Transmission electron microscopy (TEM) imaging was carried out by carbon-coated 300 square mesh copper grids (Electron Microscopy Sciences). DOX-GNR-loaded NPs, MVs, and MMNPs were left on the grid for 5 min

before being washed with 10 drops of deionized water. Each sample was then stained with 3 drops of 0.5 % uranyl acetate (Sigma Aldrich). Excess solution was absorbed with absorbent paper, and the TEM images of the samples were obtained using a High Resolution Transmission Electron Microscope (HR-TEM, JEM-3010, JEOL, Japan).

MSC membrane was dyed with 3,3′-Dioctadecyloxacarbocyanine perchlorate (DiO) before being extruded, and DOX exhibits red orange fluorence. After extrusion, cell membrane coating success was evaluated via Confocal Laser Scanning Microscope (Carl Zeiss LSM710, Zeiss, Germany).

2.7 DOX Release of MMNP

To plot DOX release profiles, 1 mg of MMNPs and DOX-GNR-loaded NPs were dispersed in 1 ml of PBS and shaked at 37 ℃. PBS buffer was changed at 3h, 6h, 10h, 16h, 24h, 48h throughout the whole dialysis process. At each predetermined time point, the solutions were centrifuged at 14,000 rpm for 30 minutes and the fluorescence of supernatant was measured.

2.8 MMNP Membrane Protein Characterization

For western blot analysis, MSC membranes were separated and suspended in a lysis buffer (10X Cell lysis buffer and 100X PMSF in DW), and protein extracts from the MSC membranes were centrifuged at 14,000 rpm and 4 ℃for 20 min. Bicinchoninic acid protein assay (Pierce Biotechnology) was used to determine the protein concentration. The protein extracts were loaded on a 10 % SDS-PAGE and transferred to a nitrocellulose membrane via an iBLOT system (Invitrogen). Protein-transffered membrane was blocked with 5 % skimmed milk in Tris-buffered saline with Tween 20 (TBS-T) for 1 hour and then incubated with primary antibodies (anti-Integrin α4, anti-Integrin β1, anti-VCAM, and anti-β actin) for another 1 hour at room temperature. The membrane was washed with TBS-T every 10 min for 5 times and incubated with anti-mouse or anti-rabbit second antibody in 5 % skimmed milk for 45 min. The membrane was washed 5 times again and the immunoreactivity was visualized.

2.9 Nanoparticle Endocytosis Analysis

The HUVECs were cultured on cover glasses in 12 well plates (10 wells, 5 x 10^4 cells / well), and four wells of the plate were incubated with TNF-α for 24 hours. The rest of cells were cultured with normal EGM-2. To coat the DOX-GNR-loaded NPs with membranes, MSCs, cultured on three 150 mm dishes, were also treated with TNF-α, and the other three 150 mm dishes of MSCs were stayed normal. MSC membranes were separated and dyed with DiO for 4 hours. After TNF-α MMNPs and MMNPs sythesis, TNF-α treated HUVEC wells were treated with TNF-α MMNPs and MMNPs in 1 mg/ml concentration. After two hours of incubation, each well was washed for two times. HUVECs were dyed with DAPI and confocal images were observed by Confocal Laser Scanning Microscope (Carl Zeiss LSM710, Zeiss, Germany).

2.10 Targeting and Photothermal Effect of MMNP on co-cultured cells

To replicate tumor vasculature and cancer near the blood vessels, HUVECs and HT1080s were co-cultured in 6 wells of a 12 well plate (5×10^4 cells / well each). Three wells were treated with TNF-α for 24 hours. TNF-α MMNPs were treated to TNF-α treated wells, and normal MMNPs were treated to normal wells for 2 hours. After two times of washing, each well was irradiated with 600 nm laser at 2 W/cm^2 power for 5 minutes. Temperature variation was recorded for every 30 s.

The cytotoxicity of HUVECs and HT1080s were evaluated with a thiazolyl blue tetrazolium bromide (MTT) assay.cells were incubated for 24 hours, washed two times with PBS, and 1 ml of MTT solution (10 % in EGM-2 medium) was added. 3 hours after, the cells were washed two times and 400 μl of dimethyl sulfoxide (DMSO) was added to each well. 100 μl of DMSO solution was transported to 96 well plate, and absorbance of each well was read at 540 nm with a plate reader.

2.11 Targeting and Photothermal Effect of MMNP on cancer cells

To replicate deeper tumor away from blood vessels, HUVECs were cultured in 15 wells of 12 transwell plate, while HT1080s were cultured in 15 wells of a 12 well plate (5 x 10^4 cells / well each). 6 wells of transwell plate were treated with TNF-α for 24 hours. TNF-α MMNPs were treated to three of TNF-α treated transwells and three of normal transwells for 2 hours. Normal MMNPs were also treated to three of TNF-α treated transwells and three of normal transwells for 2 hours. After two times of washing, each HUVEC-culturing well was irradiated with 600 nm laser at 2 W/cm^2 power for 5 minutes. Temperature variation was recorded for every 30 s.

Irradiated HUVECs were moved onto HT1080 plate. The cytotoxicity of HUVECs and HT1080s were evaluated with a thiazolyl blue tetrazolium bromide (MTT) assay.cells were incubated for 24 hours, washed two times with PBS, and 1 ml of MTT solution (10 % in EGM-2 medium) was added. 3 hours after, the cells were washed two times and 400 μl of dimethyl sulfoxide (DMSO) was added to each well. 100 μl of DMSO solution was transported to 96 well plate, and absorbance of each well was read at 540 nm with a plate reader.

3. Results and Discussion

3.1 Synthesis and characterization of DOX-GNR-PLGA nanoparticles

DOX-GNR-loaded NPs were fabricated using the w/o method. As measured by DLS, DOX-GNR-loaded NPs were found to have an diameter of 204.5 ± 51.9 nm averagely (Figure 2a). Furthermore, the loading amount of DOX and GNR per 1 mg of DOX-GNR-loaded NPs were 38.23μg and 2.8μg respectively (Figure 2b and 2c). In order to evaluate the photothermal effect of the DOX-GNR-loaded NPs, real-time infrared thermal imaging was conducted with 660 nm laser irradiation at a 2 W/cm^2 power density (Figure 2d). The temperature increase of DOX-GNR-loaded NPs was incredibly higher compared to the temperature increase of nanoparticles without GNR. 5 minutes after laser irradiation, the temperature of DOX-GNR-loaded NPs reached 50 ℃, while that of the nanoparticles without GNR was only 32.3 ℃ (Figure 2e).

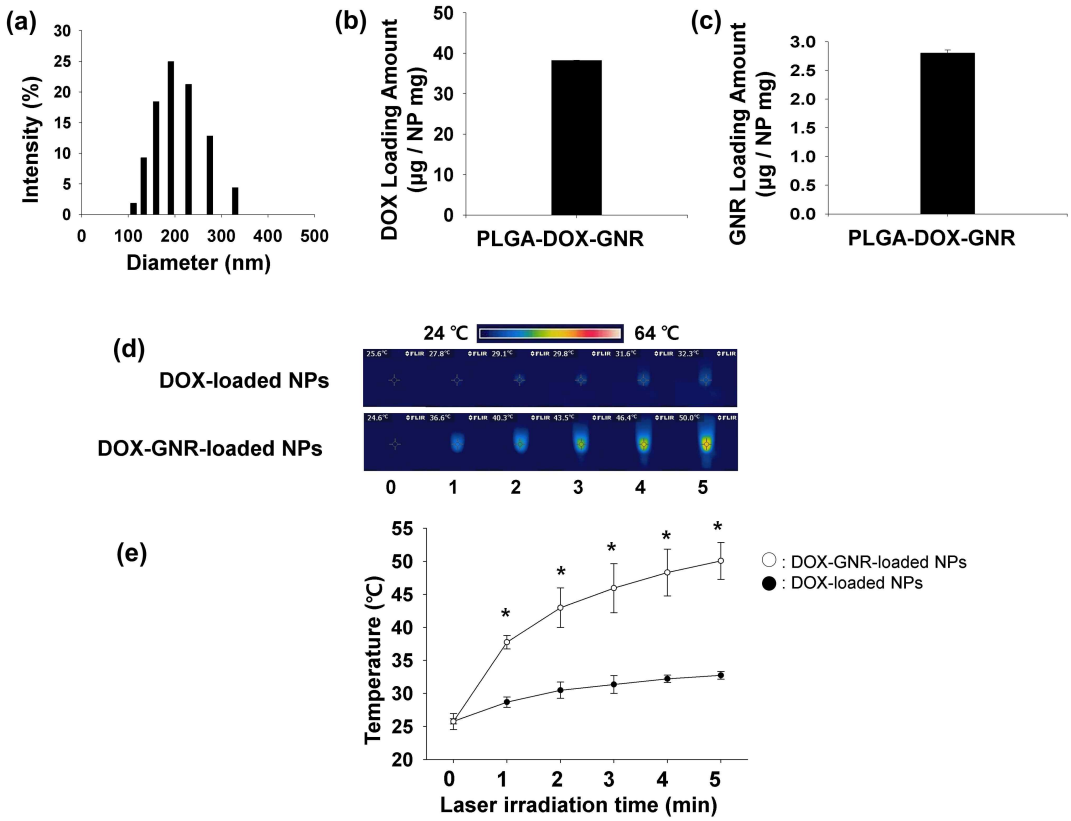

Figure 2. (a) PLGA-DOX-GNR nanoparticle size by DLS. (b) DOX loading amount per mg of DOX-GNR-loaded NPs. (c) GNR loading amount per mg of DOX-GNR-loaded NPs. (d) Real-time infrared thermal images after irradiation for 5 minutes. (e) Temperature increases of each group after 5 minute of irradiation (n = 3). * $P < 0.05$ compared to any data in DOX-loaded NPs group.

3.2 Physicochemical characterization of MMNPs

In order to synthesize MMNPs, the DOX-GNR-loaded NPs were coated with MSC membrane or TNF-α-treated MSC membrane via an extrusion method using 400nm porous polycarbonate membrane. To examine whether the nanoparticles were well coated with MSC membrane, zeta-potential of DOX-GNR-loaded NPs, MSC membrane vesicles (MVs), and MMNPs were measured (Figure 3a). While the zeta-potential of DOX-GNR-loaded NPs exhibited - 15.5 ± 0.3 mV, that of MMNPs was - 1.8 ± 0.3 mV, which is closer to the zeta-potential of MVs (-4.6 ± 0.4 mV). This result indicates that MMNPs were successfully covered with MSC membrane. We also acquired the confocal and TEM images of MMNPs to ensure whether MMNPs were well synthesized. In confocal images, MSC membranes were dyed with DIO and DOX itself is intrinsically fluorescent in red color (Figure 3b). The ratio of MMNPs to DOX-GNR-loaded NPs (the number of yellow particles compared to the number of red particles) was calculated as 69.6 % (Figure 3c). The TEM images of DOX-GNR-loaded NP, MV, and MMNP exhibited spherical shapes, Especially, membrane coating on a polymeric core appeared to have a smooth and uniform thickness under 10 nm (Figure 3d). DOX releasing plots of DOX-GNR-loaded NPs and MMNPs were described in Figure 3e.

Western blot assay was carried out to analyze the membrane protein content which is necessary for MMNPs to adhere to vessels near tumor (Figure 4). To ensure VCAM-1 and VLA-4 are stable even after subcellular fraction and ultra-centrifugation, we used proteins acquired from collected MSC membrane and TNF-α-treated MSC membrane. As in Figure 4, it is obviously shown that TNF-α treatment increased the amount of VCAM-1 and VLA-4 on MSC membrane.

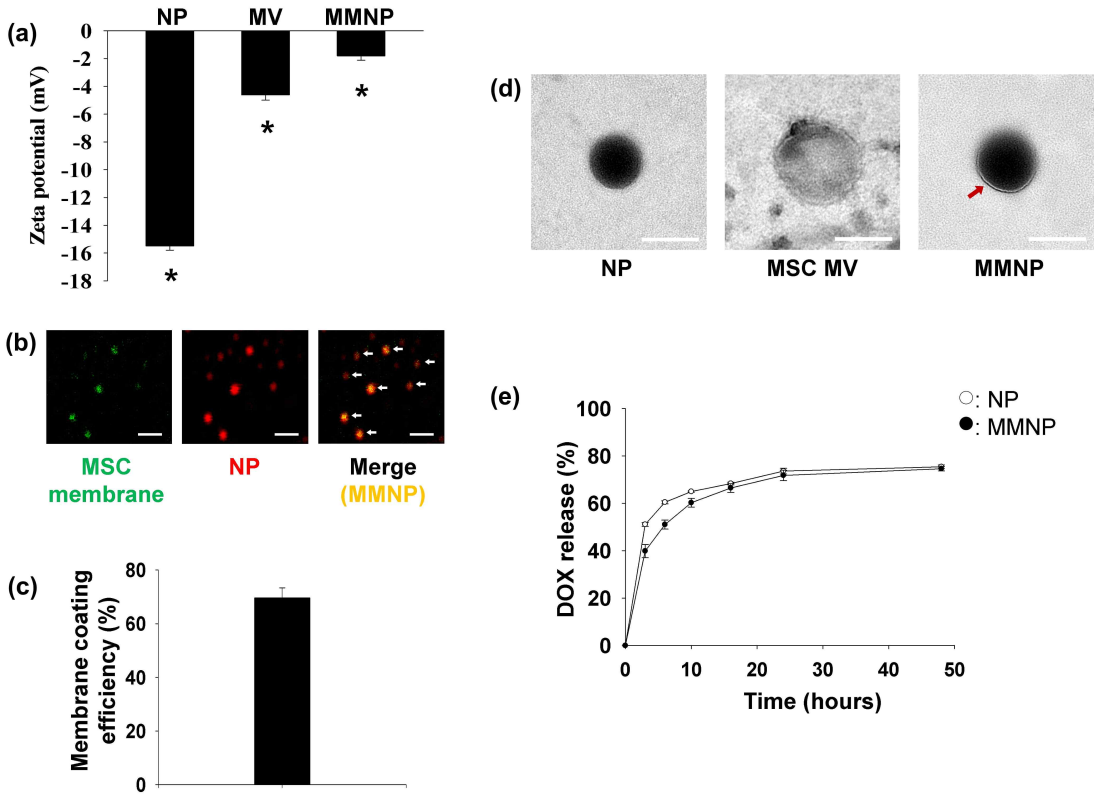

Figure 3. Characterization of MMNPs. (a) Zeta potential of DOX-GNR-loaded NP, MV, and MMNP. * $P < 0.05$ compared to any group. (b) Confocal images of synthesized MMNPs. MSC membranes were dyed with DiO (green) befor synthesis and DOX is intrinsically red fluorescent. Nanoparticles successfully coated with membranes exhibit yellow fluorescence (marked with white arrows) in the right pannel. Scale bar: 1 μm. (c) Mebrane coating yield calculated with confocal images (n = 4). (d) TEM images of DOX-GNR-loaded NP, MV, and MMNP. TEM image of MMNP shows MSC membrane layer coated on the core (marked with red arrow). Scale bar: 100nm. (e) DOX release of DOX-GNR-loaded NPs and MMNPs for 2 days.

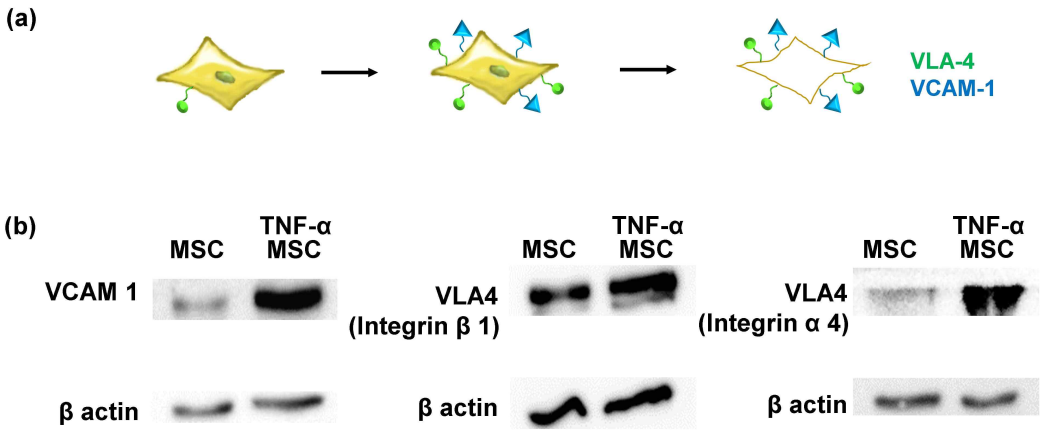

Figure 4. (a) Schem of TNF-α stimulation and membrane separation from the cell. (b) Western blot assay for MSC membrane and TNF-α treated MSC membrane, using antibodies against VCAM-1, integrin β-1, integrin α-4, and β-actin.

3.3 Endocytosis of MMNPs into HUVEC

To confirm that the TNF-α-treated MMNPs have a superior tumor-targeting effect compared to nanoparticles covered with normal MSC membrane, DOX fluorescent intensity was observed (Figure 5). HUVEC membrane was labeled with DiO (green), the nuclei of HUVECs were dyed with DAPI (blue), and DOX itself has intrinsic red fluorescence. Groups were divided in five as TNFα-treated HUVECs with TNFα-treated MMNPs (TMTH), TNFα-treated HUVECs with normal MMNPs (TMNH), normal HUVECs with TNFα-treated MMNPs (TMNH), normal HUVECs with normal MMNPs (NMNH), and just normal HUVECs. Fluorescent intensity of DOX in TMTH group was much stronger than any other groups. Especially, even TNF-α-treated MMNPs showed less effective uptake by normal HUVECs, which indicates TNF-α-treated MMNPs have an outstanding target efficiency toward blood vessel near tumor.

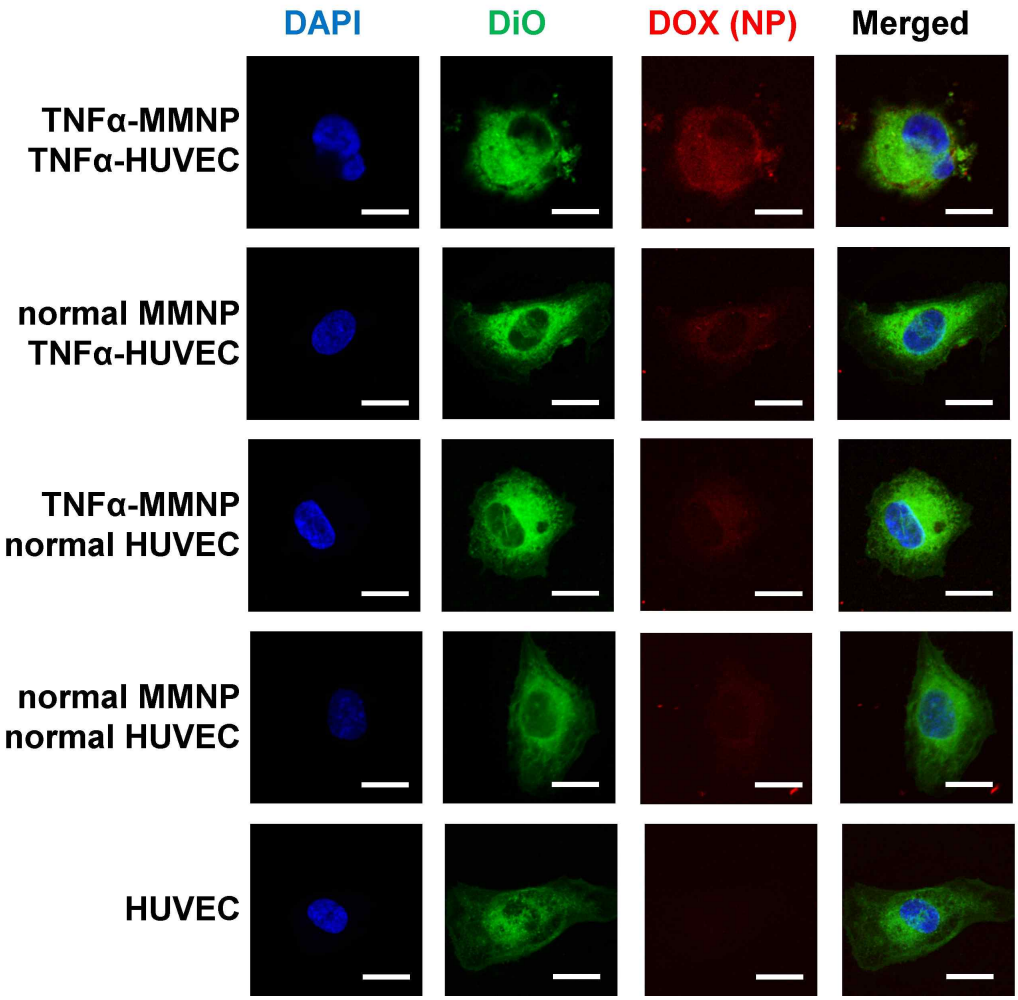

Figure 5. Endocytosis TNF-α treated MMNPs or normal MMNPs into TNF-α HUVEC or normal HUVEC. The nuclei and the membranes of HUVECs were dyed with DAPI (blue) and DiO (green) respectively. DOX is intrinsically red fluorescent. Scale bar: 20 μm.

3.4 Targeting and Photothermal Effect of MMNP

We compared the photothermal effects of TNF-α-treated MMNPs or normal MMNPs in tumor models. First of all, TNF-α-treated HUVECs and HT1080 were co-cultured in 6 wells to establish a model where blood vessels and tumor are adjacent. 2 hours after the cells were treated with TNF-α-treated MMNPs, each well were washed two times with PBS and irradiated with a 660nm laser at a 2 W/cm^2 power density for 5 minutes (Figure 6a). Normal HUVECs and HT1080 were irradiated without MMNP-treatment as a control group. The groups treated with TNF-α-treated MNPs exhibited temperature increase upto 43.0 ℃, while the temperature of the control group only reached 36.6 ℃. This result demonstrated that coating with TNF-α-treated MSC membrane enhanced tumor-targeting effect and also the photothermal capability. After irradiation, the cells were incubated 24 hours, and then the cytotoxicity of TNF-α-treated MMNPs against TNF-α-treated HUVECs and HT1080 was assessed via MTT assay (Figure 6b). Compared to normal cell, the laser-irradiated group showed 95 % of the cell viability. The MM3NP-treated and laser-irradiated group, however, exhibited 48.1 % of the cells were viable.

We next set the model for the case of deeper tumor by culturing HUVECs on transwells separated from the plates where HT1080 cells were cultured. Groups were divided as TNF-α-treated HUVECs with TNF-α-treated MMNPs, TNF-α-treated HUVECs with TNF-α-nontreated MMNPs, TNF-α-nontreated with TNF-α-treated MMNPs, and TNF-α-nontreated HUVECs with TNF-α-nontreated MMNPs. 2 hours after the HUVECs were incubated with MMNPs, the HUVECs were irradiated with a 660nm laser at a 2 W/cm^2 power density for 5 minutes (Figure 7a). In this step, transwells were located right onto HT1080 wells to avoid drug leaking. According to Figure 7a, the TNF-α-treated HUVECs with TNF-α-treated MMNP group increased up to the highest temperature of 44.2 ℃. After 2 hour irradiation, HT1080 cells were

incubated for 24 hours, and then cell viability was evaluated (Figure 7b). Compared to normal cells, TNF-α-treated HUVECs with TNF-α-treated MMNPs group exhibited 54.9 % of cell viability, meanwhile the cell viabilities of the other groups were early 70 %. Consequently, this result demonstrated that coating with TNF-α-treated MSC membrane significantly enhanced the tumor-targeting efficiency and the photothermal ability.

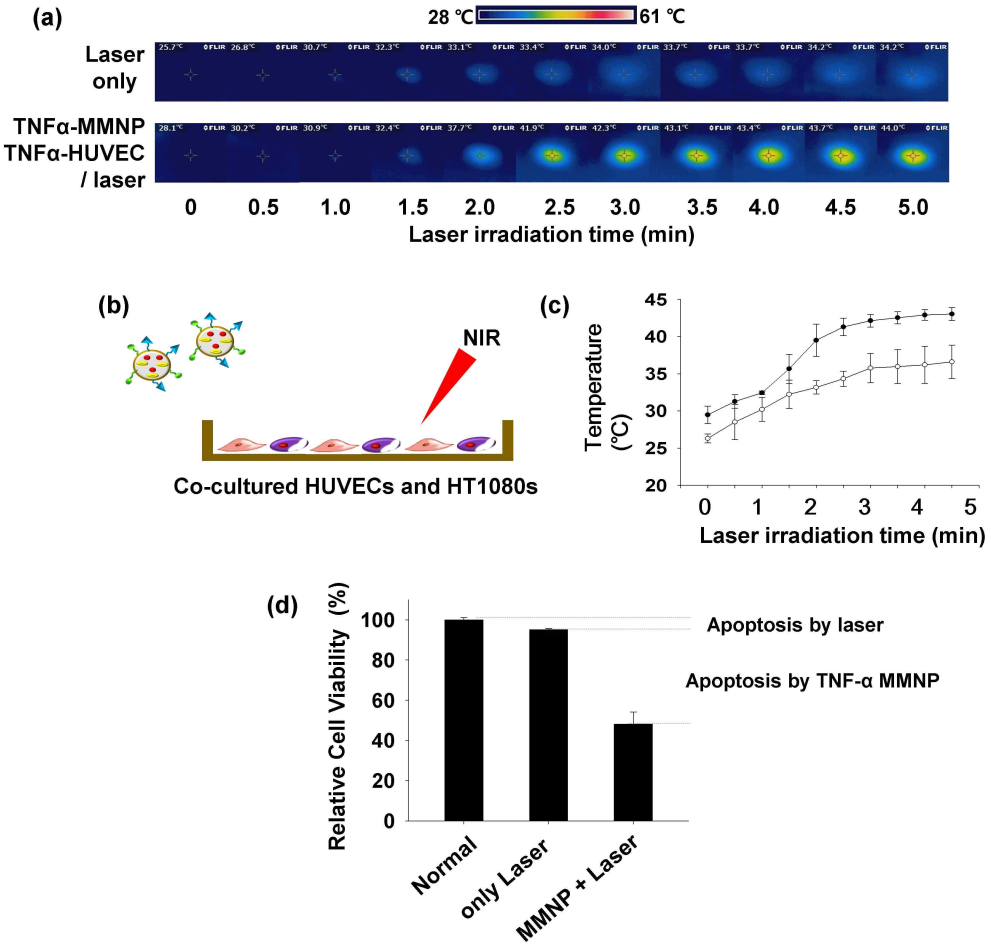

Figure 6. (a) Real-time infrared thermal images during irradiation to HUVECs or TNF-α MMNPs treated TNF-α HUVECs for 5 minutes. (b) Scheme of co-cultured HUVECs and HT 1080 treated TNF-α treated MMNPs and then infrared irradiation. (c) Temperature increases of each group after 5 minute of irradiation (n = 3). (d) The graph is a MMT assay result showing viability of normal HUVECs and HT 1080s, irradiated HUVECs and HT 1080s, and HUVECs and HT 1080 treated TNF-α treated MMNPs with infrared irradiation.

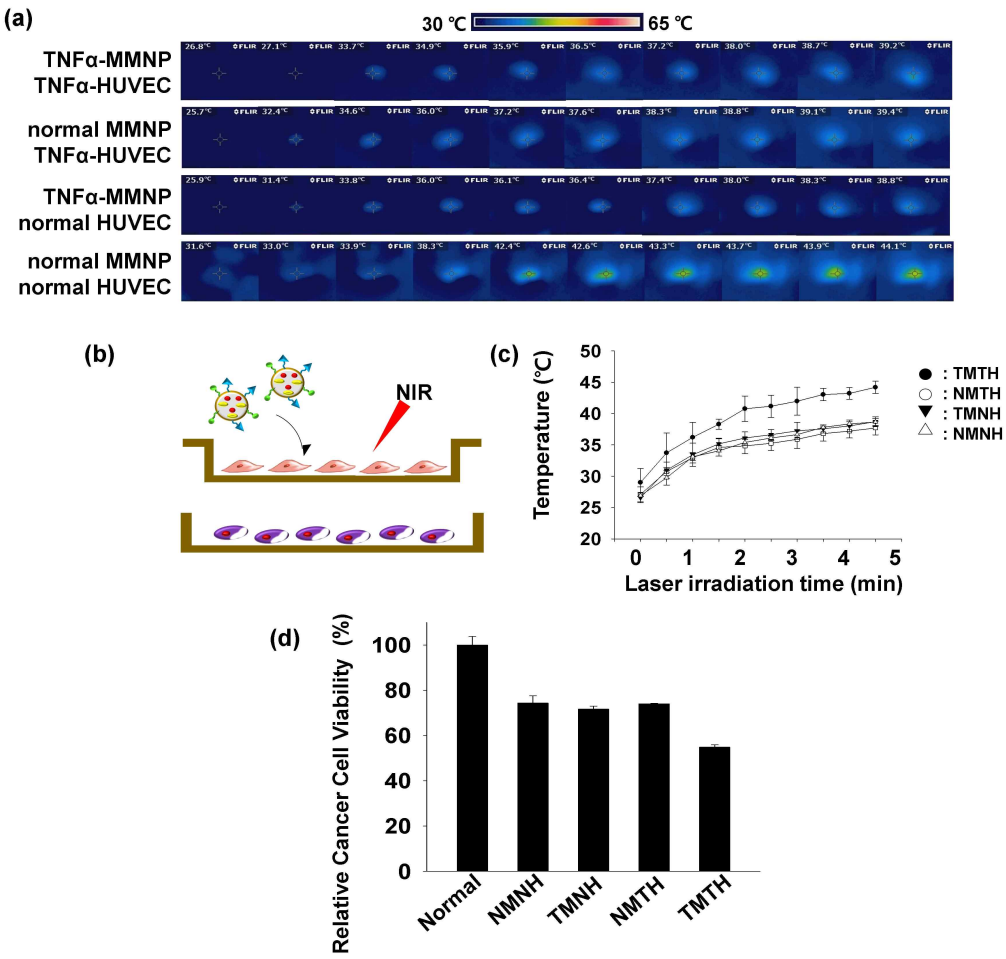

Figure 7. (a) Real-time infrared thermal images after irradiation for 5 minutes. (b) Scheme of HUVECs and HT 1080s. HUVECs were cultured on transwells. (c) Temperature increases of each group after 5 minute of irradiation (n = 3). TMTH: TNF-α treated HUVECs with TNF-α treated MMNPs, NMTH: TNF-α treated HUVECs with TNF-α untreated MMNPs, TMNH: HUVECs with TNF-α treated MMNPs, NMNH: HUVECs with TNF-α untreated MMNPs. (d) Relative cancer cell viability via MTT assay.

4. Conclusion

Herein, we demonstrated that TNF-α treatment increases VCAM-1 and VLA-4 expression on MSC surface. TNF-α treated MSC membranes were coated on DOX-GNR-loaded NPs, and TNF-α MMNPs exhibited excellent tumr vasculature targeting capability. Irradiation allowed apoptosis of endothelial cells and cancer cells near blood vessels. Furthermore, DOX-GNR-loaded NPs flowed into deeper cancer cells and caused cell death after irradiation in vitro model. This therapy may be used in vivo system in future for cancer treatments.

5. References

[1] Qiong Xiao, Shi-kun Wang, Hua Tian, Li Xin, Zhi-geng Zou, Li-yan Wang, et al. TNF-a Increases Bone Marrow Mesenchymal Stem Cell Migration to Ischemic Tissues. Cell Biochem Biophys. 2012; 62:409 - 414.

[2] Hiroshi Yagi, Alejandro Soto-Gutierrez, Biju Parekkadan, Yuko Kitagawa, Ronald G. Tompkins, Martin L. Yarmush, et al Mesenchymal Stem Cells: Mechanisms of Immunomodulation and Homing. Cell Transplant. 2010; 19(6): 667 - 679.

[3] Michael R, Loebinger, and Sam M Janes. Stem cells as vectors for antitumour therapy. Thorax. 2010. April; 65(4): 362 - 369.

[4] E Spaeth, A Klopp, J Dembinski, M Andreeff and F Marini. Inflammation and tumor microenvironments: defining the migratory itinerary of mesenchymal stem cells. Gene Therapy. 2008; 15: 730 - 738.

[5] Brigitte Ru¨ ster, Stephan Go¨ ttig, Ralf J. Ludwig, Roxana Bistrian, Stefanie Mu¨ ller, Reinhard Henschler, et al. Mesenchymal stem cells display coordinated rolling and adhesion behavior on endothelial cells. Blood. 2006; 108: 3938-3944.

[6]. Ryosuke Uchibori, Tomonori Tsukahara, Hiroyuki Mizuguchi, Yasushi Saga, Masashi Urabe, Keiya Ozawa, et al. NF-kB Activity Regulates Mesenchymal Stem Cell Accumulation at Tumor Sites. Cancer Research. 2013; 73: 364-372.

[7] Stuart M. Grieve, Jacob Lønborg, Jawad Mazhar, Timothy C. Tan, Edwin Ho, Gemma A, et al. Figtree Cardiac magnetic resonance imaging of rapid VCAM-1 up-regulation in myocardial ischemia - reperfusion injury. Eur Biophys J. 2013; 42: 61 - 70.

[8] Antoine E. Karnoub, Ajeeta B. Dash, Annie P. Vo, Andrew Sullivan, Mary W. Brooks, Robert A. Weinberg, et al. Mesenchymal stem cells within tumour stroma promote breast cancer metastasis. 2007; 449(7162): 557-63.

[9] Wei Zhu, Ling Huang, Yahong Li, Xu Zhang, Jianmei Gu, Wenrong Xu, et

al. Exosomes derived from human bone marrow mesenchymal stem cells promote tumor growth in vivo. Cancer Letters. 2012; 315: 28-37.
[10] Ronnie H. Fang, Che-Ming J. Hu, Brian T. Luk, Weiwei Gao, Jonathan A. Copp, Liangfang Zhang, et al. Cancer Cell Membrane-Coated Nanoparticles for Anticancer Vaccination and Drug Delivery. Nano Lett. 2014; 14: 2181－2188.
[11] Santosh Aryal, Che-Ming J Hu, Ronnie H Fang, Diana Dehaini, Cody Carpenter, Liangfang Zhang, et al. Erythrocyte membrane-cloaked polymeric nanoparticles for controlled drug loading and release. Nanomedicine. 2013; 8(8): 1271 - 1280.
[12] Che-Ming J. Hu, Li Zhang, Santosh Aryal, Connie Cheung, Ronnie H. Fang, and Liangfang Zhang. Erythrocyte membrane-camouflaged polymeric nanoparticles as a biomimetic delivery platform. Proc Natl Acad Sci USA. 2011; 108(27): 10980-5.
[13] Alessandro Parodi, Nicoletta Quattrocchi, Anne L. van de Ven, Ciro Chiappini, Michael Evangelopoulos, Ennio Tasciotti, et al. Biomimetic functionalization with leukocyte membranes imparts cell like functions to synthetic particles. Nat Nanotechnol. 2013; 8(1): 61 - 68.
[14] Weiwei Gao and Liangfang Zhang. Coating nanoparticles with cell membranes for targeted drug delivery. J Drug Target. 2015; 23(7 - 8): 619 - 626.
[15] Seokyung Kang, Suk Ho Bhang, Sekyu Hwang, Jeong-Kee Yoon, Sungjee Kim, Byung-Soo Kim, et al. Mesenchymal Stem Cells Aggregate and Deliver Gold Nanoparticles to Tumors for Photothermal Therapy. ACS Nano. 2015; 9(10): 9678-90.
[16] Chih-Hang Chu, Yu-Chao Wang, Lin-Ai Tai, Li-Chen Wua and Chung-Shi Yang. Surface deformation of gold nanorod-loaded poly(DL-lactide-co-glycolide) nanoparticles after near infrared irradiation: an active and controllable drug release system. J. Mater. Chem. 2010; 20: 3260 - 3264.
[17] Jason Park, Peter M. Fong, Jing Lu, Kerry S. Russell, Carmen J. Booth, Tarek M. Fahmy, et al. PEGylated PLGA nanoparticles for the improved delivery of doxorubicin. Nanomedicine. 2009; 5(4): 410 - 418.

[18] Huiyul Park, Jaemoon Yang, Jaemin Lee, Seungjoo Haam, In-Hong Choi, and Kyung-Hwa Yoo. Multifunctional Nanoparticles for Combined Doxorubicin and Photothermal Treatments. ACS NANO. 2009; 3(10): 2919-2926.

요약 (국문초록)

암 치료를 위한 세포막으로 코팅된 독소루비신과 금나노로드가 함유된 PLGA 나노입자 개발

줄기세포는 자기 재생과 분화 능력 등과 같은 우수한 특성에 의해 바이오 분야에서 활발히 연구에 사용되고 있다. 다양한 특성 중에서도 줄기세포는 부상 조직 또는 암 주변으로 유도되는 특성이 있어 암 치료를 위한 약물 전달에 활용이 가능하다. 그러나 줄기세포 자체 또는 줄기세포에서 유도된 엑소좀은 암 성장을 유도하는 작용을 한다는 단점이 있어, 줄기세포를 통한 약물 전달이 오히려 질병을 악화시키는 가능성이 존재한다. 본 연구에서는 줄기세포의 단점은 제외하고 장점만을 이용하고자, 줄기세포의 세포막을 분리하여 이를 나노입자에 도포하는 방법을 고안하였다. 나노입자는 독소루비신과 금나노로드가 포함하는 poly(lactic-co-glycolic acid) (PLGA) 나노입자 (DOX-GNR-loaded NPs)로 합성하였다. 암 주변 혈관세포의 표면은 very late antigen-4 (VLA-4)과 vascular cell adhesion molecule-1 (VCAM-1)가 일반 혈관세포에 비하여 많이 발현되며, 종양괴사인자 (TNF-α)를 처리한 MSC의 세포막에서도 VLA-4와 VCAM-1의 양이 증가한다. VCAM-1은 VLA-4의 리간드로 인력이 작용하므로, TNF-α 처리한 줄기세포의 세포막으로 나노입자를 코팅 (TNF-α MMNPs)함으로써 입자의 암 타겟팅 효과를 향상시켰다. 인비트로 실험은 혈관과 암이 인접한 부위와 혈관으로부터 멀어진 더 깊숙한 암 부위 두 가지 모델을 설정하고자, 혈관세포와 암세포의 혈관세포를 공동 배양한 실험과 트랜스웰에 분리하여 배양한 실험을 진행하였다. TNF-α MMNPs를 처리한 후, 660nm의 레이저를 2W/cm^2 출력으로 투사한 결과, 각 모델에서 세포의 온도가 43.0 ℃와 44.2 ℃로 상승하였다. 공동 배양된 혈관세포와 암세포는 48.1 % 만이 생존하였으며, 두 세포를 분리하여 배양한 경우, 암세포 사멸 정도가 45.1% 에 달하였다.

본 연구를 통해 개발된 TNF-α 처리 줄기세포막 코팅 나노입자는 우수한

암 타겟팅 능력과 근적외선에 의한 발열 특성을 보유하고 있음을 확인하였다. 또한, 본 연구의 나노입자를 전달함으로써 암 주변 혈관과 인접 암세포의 사멸은 물론, 깊숙한 암 조직까지 세포 사멸을 야기할 수 있음을 인비트로에서 볼 수 있었다.

향후에 TNF-α 처리 줄기세포막 코팅 나노입자를 인 비보에 적용함으로써 나노입자의 유용성을 확인할 수 있을 것이며, 암 이외의 다양한 질병에도 폭넓게 응용이 가능할 것으로 기대된다.

주요어 : 암 치료, 종양 혈관, 종양괴사인자, 줄기세포막, 세포막 도포, 약물전달 시스템

학번 : 2014-22612